

AN UNSTRUCTURED WAVE DRAG CODE FOR PRELIMINARY DESIGN OF FUTURE SUPERSONIC AIRCRAFT

Sriram K. Rallabhandi* and Dimitri N. Mavris†
Aerospace Systems Design Lab, Georgia Tech, Atlanta

Abstract

In a preliminary design environment, the designer needs to have freedom to quickly evaluate different configurations and come up with the most promising configuration. In the supersonic regime, most linearized codes that are available today can only handle specific shapes and configurations. These codes only aid in optimizing conventional configurations and do not span the entire space of possible shapes, which include revolutionary and unconventional configurations. This paper proposes using a set of GNU libraries and analyses codes to overcome the shortcomings of the legacy codes. It is known that any surface can be discretized into triangles using efficient Delaunay triangulation algorithms. The proposed method involves creating a triangulated aircraft from a generic CAD environment, using the set of geometric libraries and then performing necessary surface operations for the desired result, which in our case is the calculation of the wave drag. Linearized methods for wave drag estimation call for the calculation of the intercepted areas of the aircraft with a Mach cone and the GNU libraries help us in obtaining these areas. Finally, in order to validate the code, the new code is used to compute the wave-drag of a Sears-Haack body and F-16 and the results are compared to the results from AWAVE, the Harris Wave Drag program.

Introduction

The design of an efficient aircraft is dependent on the availability of rapid and sufficiently accurate theoretical and computational methods for aerodynamic analysis. Proper effect of the aerodynamic influence in the initial phases of design should be accurately predicted so that the best configuration can be selected. Traditionally, preliminary supersonic aerodynamic analysis has relied on various linearized and modified linearized¹⁻³ methods. In addition to these

programs, analysis of supersonic flight needs pressure wave propagation⁴ routines. The linearized sonic boom theory is mostly based on the work of Whitham⁵ and Walkden.⁶ Various concepts of sonic boom theory have been introduced⁷⁻⁸ and sonic boom minimization⁹⁻¹⁰ has also been investigated.

Even though it is desired to use computational fluid dynamics much earlier in the design, today's computational power does not allow a quick and easy prediction of the required aerodynamic data. This is the reason people still rely on fast linearized models. However, as the aircraft configuration assumes unconventional shapes in the design environment, most of the linearized legacy codes fail to produce aerodynamic data to the necessary accuracy or detail. Moreover, input to many of these legacy codes is generally in the form of awkward control cards and many times the actual geometry needs to be tweaked for the code to handle the geometry. Since geometry holds the key to designing better aircraft, a tool or analysis code is needed that can perform the aerodynamic analysis without any assumptions pertaining to the geometry of the aircraft. The linearized codes have to be constantly upgraded to be able to correctly model, at-least to the first order, the effects of revolutionary aircraft shapes. To increase the fidelity of the analysis, any proposed tool should be capable of doing complex three dimensional geometric operations rather than being limited to planar approximations. In this study we attempt to improve the capability of the traditional wave drag method so that the new code can handle arbitrary geometries accurately. In doing so, we also obtain other important parameters which will prove useful in the later stages of the aerodynamic design.

Before proceeding to discuss a new program, let us look further into the shortcomings of the traditional wave drag code that is used in most analyses today. Harris wave drag code was developed by Boeing and NASA Langley for the determination of fuselage cross-sections which yield minimum wave drag. This is achieved by enforcing the supersonic area rule, which employs Von-Karman's slender body formula. Apart from approximating the geometry in terms of awkward control cards, this program does not perform a smooth transition between the fuselage and wing root

*Graduate Research Assistant, Student member AIAA

†Associate Professor, Boeing chair for Advanced systems design, Associate Fellow AIAA

Presented at the 33rd Fluid Dynamics Conference and Exhibit, Orlando, Florida, June 23-26, 2003. Copyright ©2003 by Sriram Rallabhandi, D.N. Mavris, Published by American Institute of Aeronautics and Astronautics, Inc. with permission.

chord causing holes or doubly accounted areas. The extreme left part of figure 1 shows the actual wing-fuselage combination. The next two parts show the approximation in AWAVE which causes gaps or duplicates area. The reason for this is that the program can only handle straight wing sections and has no strategy to deal with the component intersections. This leads to an incorrect area and volume distribution resulting in an over-prediction of the wave drag. Since AWAVE deals with crude approximations of conventional geometries, coke bottled fuselages as well as interesting concepts like joined-wing, channel-wing and oblique-wing cannot be handled with this setup.

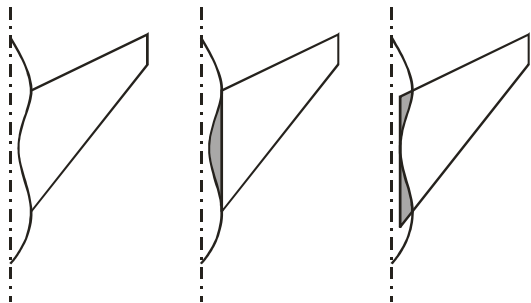


Fig. 1 Poor Aircraft Numerical Definition

Using the same theoretical basis as used in AWAVE, we have developed a code which accepts any arbitrary configuration as input and computes the wave drag of the configuration. The process involves triangulating the surface to obtain a surface grid, calculating the Mach-cone intersected areas of the configuration, obtaining the second derivatives of the area distribution and performing numerical gaussian quadrature to obtain the wave drag and F-function. The surface grid can be used as a first step to create volume grids and used for higher fidelity analysis. The F-function can be used for shape optimization studies and Sonic Boom analysis.

Formulation

Using linearized theory, it has been shown⁷ that the wave drag of an aircraft in supersonic flight is the same as the wave drag of an equivalent body of revolution having the same cross sectional area distribution as the aircraft. The equivalent body has contributions from the volume as well as lift. Estimation of the equivalent area due to volume involves the area of the aircraft intercepted by the Mach cone. Equivalent area due to lift can be estimated by using a linearized lift analysis program like Mach-box method or accurate non-linear CFD methods. However, in this study we are concerned only with the equivalent area due to volume. In the next few paragraphs we present the formulation of a wave drag prediction environment which uses a higher degree of geometric abstraction than has been

used in many of the preliminary aerodynamic codes. The wave drag of a slender body¹² is given by equation 1

$$D_w = \frac{-\rho U^2}{4\pi} \int_0^l \int_0^l S''(x_1) S''(x_2) L n |x_1 - x_2| dx_1 dx_2 \quad (1)$$

where ρ is the free stream density, U is the free stream velocity, $S''(x_1), S''(x_2)$ are the second derivatives of the area distribution with respect to the integration parameters, x_1, x_2 , which are the locations along the axis of the aircraft. To obtain an estimate of the wave drag of any configuration, we need an accurate representation of the second derivative of the intercepted areas. Although the area distribution is continuous along the fuselage axis, numerically we obtain the area only at certain finite number of points along the axis. It is important to maintain a sufficient resolution of the points along this axis. Failure to do so may lead to numerical round-off errors due to increased error in the second derivative calculation. As in any approximation theory, a very fine resolution may cause numerical precision errors. Thus, the resolution should be fixed so as to reduce precision errors and avoid round-off errors.

Once the second derivative of the area distribution has been obtained, we can perform a numerical quadrature to obtain the wave drag provided we know the flight conditions of the vehicle. In addition to the wave drag, we can also compute the F-function which is defined as:

$$F(x) = \frac{1}{2\pi} \int_0^x \frac{S''(t)}{(t-x)^{1/2}} dt \quad (2)$$

Calculation of F-function is important because it has been shown that the disturbance pressure away from a supersonic aircraft can be obtained in terms of the F-function as:

$$\delta p = p_0 \frac{\gamma M^2 F(x - \beta r)}{(2\beta r)^{1/2}} \quad (3)$$

where δp is the disturbance pressure, p_0 is the undisturbed ambient pressure, x is the axial co-ordinate, M is the Mach number, β is the Prandtl-Glauert factor, F is the F-function defined in equation 2 and r is the radius vector of the point of interest from the aircraft. Thus, F-function acts as an acoustic source term for the pressure signature propagation. Gaussian quadrature has been used to carry out most of the numerical integrations in this study because of its simplicity.

Geometry generation

With the procedure now well understood, we should be able to create and analyze a gamut of configurations in a short amount of time. This calls for efficient

surface parameterization techniques which can lead to efficient surface generation and automation. In this study, however, we use Rapid Aircraft Modeler (RAM), which is a conceptual level CAD environment developed at NASA Ames. RAM is capable of generating arbitrary aircraft shapes in a short amount of time for any concept by simply adjusting parameters associated with each component as shown in figure 2. RAM can be easily automated, run across platforms, is intuitive and flexible.

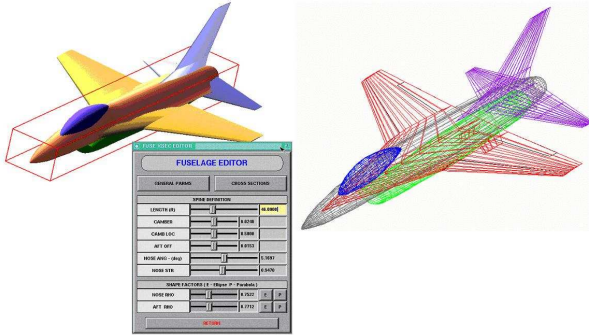


Fig. 2 RAM Concept to Wire-frame

Surface Discretization

Once a RAM model has thus been generated, we then have to discretize the surface in such a way to carry out further analysis. A very useful library called GNU triangulated surface library (GTS)¹¹ is available online from gts.sourceforge.net and is used to perform surface operations on the aircraft. Our program reads one component at a time from the RAM input file and operates on it to triangulate it. For any geometry there are openings at locations such as engine inlet and wing tips and we call these openings as holes (See figure 3). Care is taken to fill such holes with triangles so that we have a closed component to operate on.

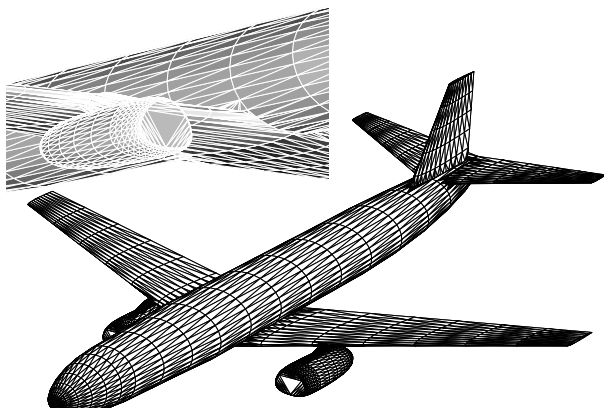


Fig. 3 Filling the Engine hole for a sample aircraft

As each additional component is read, its holes are filled and the surface is triangulated and combined with the already triangulated components using surface boolean operations to form a single unit. Thus, a RAM aircraft model as shown in figure 4 is stitched from a collection of components into a single entity. By doing so, we could eliminate the duplicated areas and volumes which would otherwise have led to an incorrect area distribution as in Harris wave drag program.

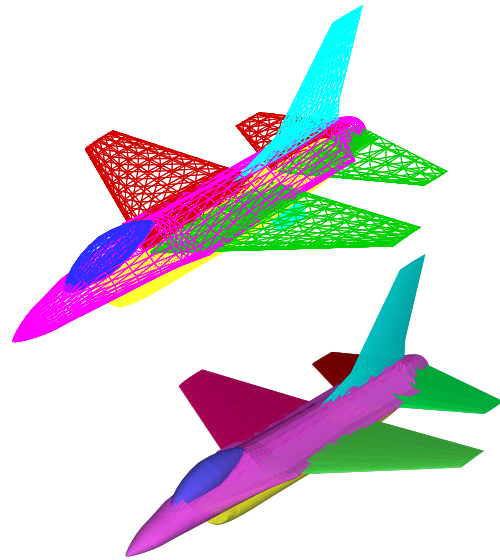


Fig. 4 Different overlapping components of an aircraft

GTS provides a simple object-oriented structure giving easy access to the topological properties of the surfaces and performs robust union, intersection and difference operations on three dimensional surfaces. Surface boolean operations within GTS perform an efficient job of calculating the three dimensional curve of intersection between components and cropping the surfaces beyond this curve. As different components are combined, GTS performs efficient re-triangulation of the new surface. After running through all the components in the RAM input file, we have a complete triangulated aircraft as shown in figure 5. The quality of the triangular grid determines the accuracy of the solution obtained because a finer triangulation is always a better approximation of complex shapes than a coarser triangulation. Thus, sufficient care is taken to make sure the triangulation is good. Apart from providing an efficient discretization scheme, the unstructured triangular grid can be used in other high fidelity analysis such as an unstructured grid solver or

an unstructured panel code for conceptual lift analysis.

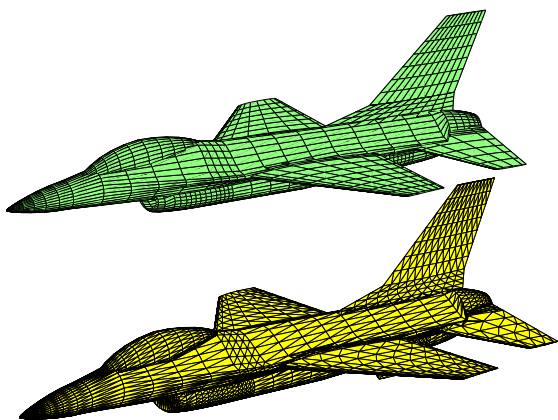


Fig. 5 Wire-frame to Triangulated Surface

Having obtained the triangulated geometry, we then generate Mach cones along the axis of the fuselage with the free-stream Mach number as an input parameter. The free stream Mach number determines the half angle of the Mach cone. According to slender body theory and equivalent body assumption, the aircraft area intersected by the Mach cone at various locations on the aircraft axis is the area that affects the wave drag computation, not the actual cross sectional area of the aircraft. To obtain the equivalent area distribution, the aircraft axis is discretized into various sections to obtain reasonable accuracy. A Mach cone is generated using GTS at the first location and the aircraft area intercepted by this cone is then determined by performing intersection operation over the surfaces. The Mach cone is gradually translated along the axis and the intersected area at each location is determined to obtain the distribution of the equivalent area due to volume of the aircraft.

Realization

With all the working details in place, we now demonstrate how the present code is used on a Sears-Haack body and an F-16 aircraft. Sears-Haack body was chosen because we can compare the results of the present code with the exact analytical expressions of its area distribution and drag coefficients. F-16 was chosen to show the strength of the method in dealing with complex geometries.

Preprocessing of a Sears-Haack Body

A Sears-Haack body is a slender body of revolution pointed at both ends, that corresponds to the minimum wave drag for given volume and length, of a linear distribution of sources at supersonic speeds. The area distribution of the Sears-Haack body is analytically given by equation¹² 4.

$$S(\theta) = \frac{4V}{\pi l} (\sin(\theta) - \frac{1}{3} \sin(3\theta)) \quad (4)$$

Figure 6 presents a triangulated Sears-Haack body. The degree of refinement of the body is under the control of the user, so the user can increase the number of radial or axial points in order to increase the accuracy of the final results.

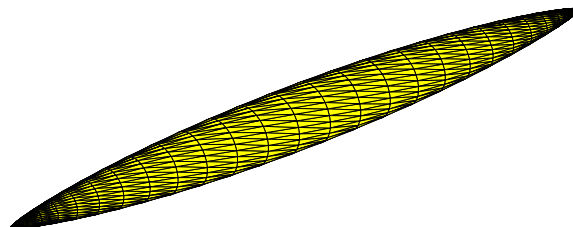


Fig. 6 Triangulated Sears-Haack body

This geometry was run at different Mach numbers and the following figures show the distribution of the area and it's second derivative for a Mach number 1.0. From Figure 7 it can be seen that at M=1.0, the maximum cross-sectional area occurs at the midpoint. The data exactly matches with the analytical expression for the area distribution. Except at the end points where there is a steep change in the area, the second derivative of area takes almost a constant value through the length of the body as shown in figure 8. This is because a quadratic curve is a good approximation to the area distribution of this body.

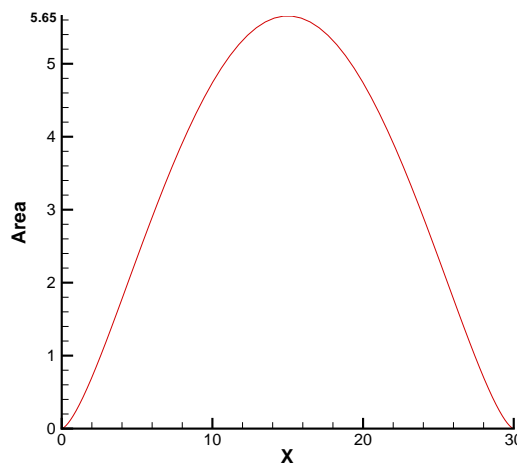


Fig. 7 Equivalent Area distribution for Sears-Haack body at M=1.0

Although the above procedure can be done for any Mach number, one has to keep in mind that the validity of linearized approximation decreases as the mach number increases beyond 1.0. The area distribution and its second derivative at Mach number 2.0 are shown in the next two figures. It can be clearly seen

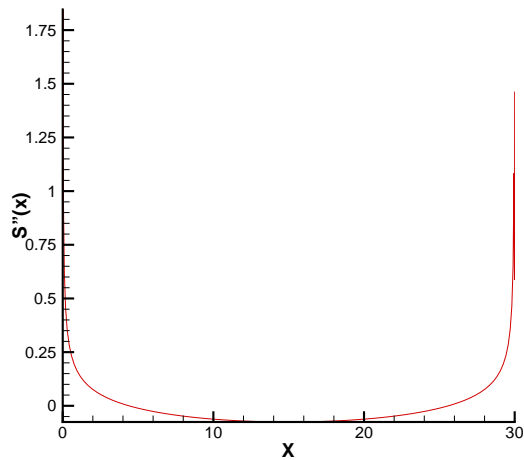


Fig. 8 Second derivative of the area distribution for the Sears-Haack at M=1.0

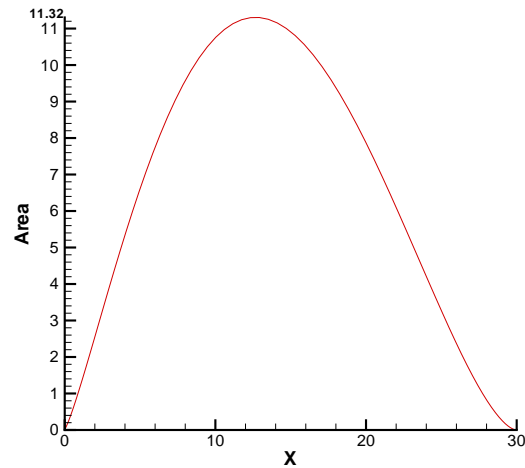


Fig. 9 Mach-cone intercepted Area distribution for Sears-Haack body at M=2.0

from figure 9 that as the Mach number increases, the magnitude of the Mach cone intercepted area increases and the peak in the area distribution shifts in the upstream direction due to the nature of the supersonic flows. However, the equivalent body area distribution is obtained by taking a normal component of the intercepted area. Figure 10 shows that the equivalent area remains the same as obtained for the case M=1.0. It can be seen from figure 11 that once again the second derivative is almost constant along the length of the body except at the ends with almost the same magnitude throughout the length as was the case for M=1.0. Since the wave drag depends on the distribution of the second derivative of area, we can expect the drag coefficient of a Sears-Haack body to be independent of the Mach number. We can now proceed to compute the F-function and drag values by performing numerical integration.

Preprocessing of F-16 aircraft

The geometry of F-16 is quite complex with an engine, horizontal and vertical stabilizers and ventral fins. A triangulated F-16 is obtained as explained in an earlier section and is shown in figure 12. In this paper, we demonstrate the results only at a Mach number of 2.0. We obtain the equivalent area distribution of this aircraft through the Mach cone intersections as described in the previous section. At this Mach number, figure 13 shows the Mach cone cuts of this aircraft. Towards the front of the aircraft, there is gradual increase in the intercepted area due the increasing radius of the fuselage and the presence of the canopy. As the Mach cone reaches a certain point on the fuselage axis, there is a contribution from the wings. However, notice that the Mach cone intercepted sections can be more than one disjointed sections at any location and the equivalent area contribution comes from the sum

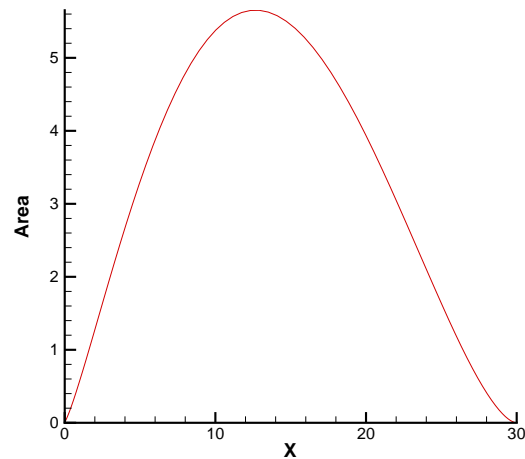


Fig. 10 Equivalent area distribution for the Sears-Haack body at M=2.0

of these sectional areas. Towards the end, there is contribution from the vertical tail and horizontal tail as well.

We thus obtain the equivalent area due to volume and its second derivative. Figure 14 shows the area distribution obtained for this free stream Mach number. The various humps seen in the figure correspond to the cumulative effect of the presence of the canopy, wings, vertical tail and horizontal tail. The engine capture is subtracted from the area because air flows through the engine inlet and not around it.

Figure 15 shows the second derivative of the area distribution of this aircraft. The figure shows the possibility of numerical errors creeping into the analysis method due to finite difference approximations, causing some jumps in this distribution at the cusp location in the area distribution. The Harris wave drag code

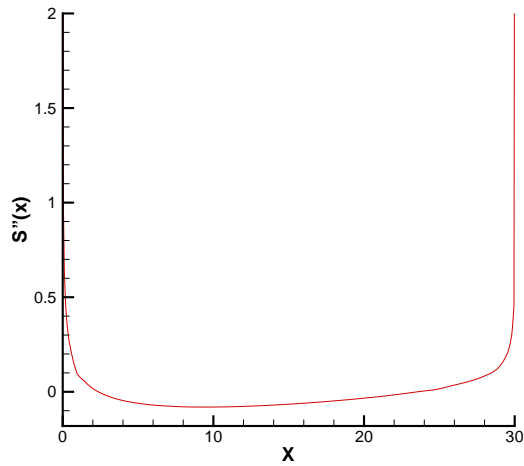


Fig. 11 Second derivative of the area for the Sears-Haack body at M=2.0

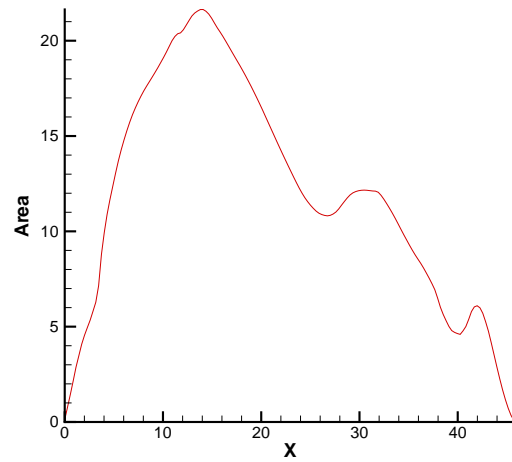


Fig. 14 Equivalent Area distribution of F-16 at M=2.0

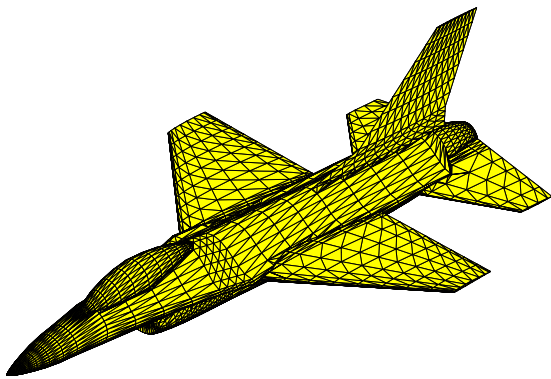


Fig. 12 Triangulated F-16

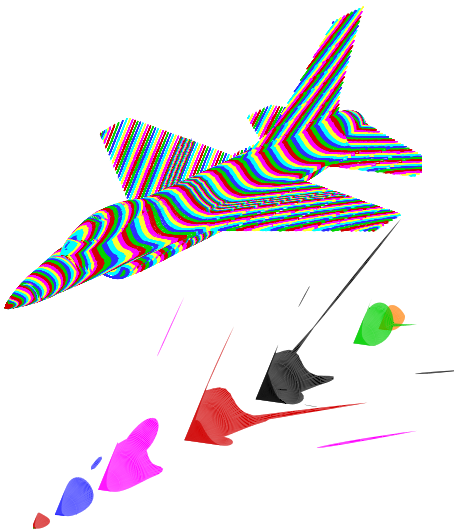


Fig. 13 Mach cone cuts of F-16 at M=2.0

does not have this problem because it deals with each component separately and adds up the second derivative of the areas of each component to arrive at the derivative area distribution of the whole aircraft. This inherently takes care of the cusps within the area distribution. In the present approach, this problem can be overcome by a clever strategy of identifying when such a cusp occurs and avoiding the cusp in the finite difference stencil by switching to an appropriate finite difference scheme. However, it is quite difficult to identify such a cusp when it occurs and so has not been implemented in the current code.

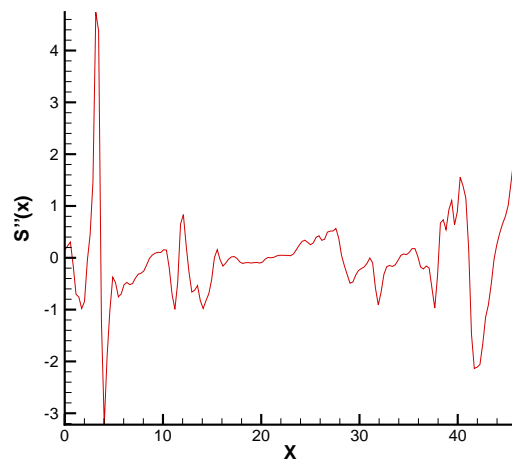


Fig. 15 Second derivative Area distribution of F-16 at M=2.0

Demonstration and Results

Finally, after having done all the necessary preprocessing we are at a position to start analyzing the results. The first part of this section will provide the

results on a Sears-Haack body and the next part for the F-16 aircraft.

Results and discussion on Sears-Haack body

The analytical expression for the wave drag of a Sears-Haack body is given by equation 5

$$D_w = \frac{64V^2}{\pi l^4} \rho U^2 \quad (5)$$

where V is the volume of the Sears-Haack body, l is the length, ρ is the free stream density and U is the free stream velocity.

The drag coefficient based on the maximum cross-sectional area is given by equation 6

$$C_{Dw} = \frac{24V}{l^3} \quad (6)$$

For all the figures provided here, the volume of the Sears-Haack body has been taken as 100.0 and the length as 30.0 with consistent units. This gives the exact drag coefficient as 0.0888. Using our code, we obtain drag coefficients of 0.089 and 0.081 for Mach number of 1.0 and 2.0 respectively. Thus, as expected, the drag coefficient is independent of Mach number for this body. The values obtained from Harris wave drag program match almost exactly with the results we obtain from our code.

Figure 16 shows the F-function of the Sears-Haack body at $M=1.0$ and figure 17 shows the F-function at $M=2.0$. Notice the presence of the sharp increase at the front and towards the end of the body. For a complex aircraft, these peaks will be pronounced and upon propagation through the atmosphere lead to the typical N wave structure usually obtained from a Sonic-Boom module.

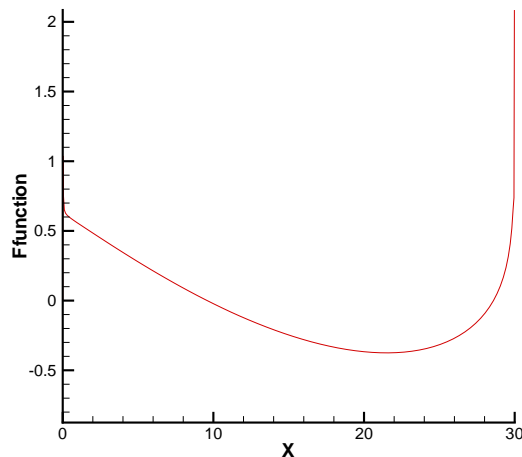


Fig. 16 F-function of Sears-Haack body at $M=1.0$

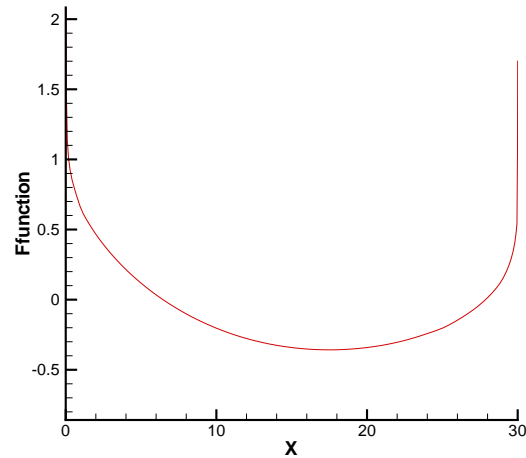


Fig. 17 F-function of Sears-Haack body at $M=2.0$

Results and discussion on F-16 aircraft

For a full aircraft configuration, since we do not have any analytical expression for drag, we have decided to use Harris wave drag program to run at the Mach number of interest and make comparisons with the data we obtain. Within the limitations of the Harris code, we created an input file to reflect the geometry of F-16 and analyzed at a Mach number of 2.0 giving the wave drag coefficient as 0.3893 with a reference area of 288.8. Using our code, we obtain a drag coefficient of 0.0357. Though there is no easy way to validate this value, we believe that the Harris wave drag code far over-predicts the drag due the area duplication and possible presence of gaps in the configuration. A thorough validation should include wave drag results from a wind tunnel experiment or from a higher fidelity analysis. However, since the physics of this method is quite simple and the limitation of Harris code with respect to complex shapes is well known, it is reasonable to say that our code does a better job when dealing with complex shapes.

Conclusions and future work

There are some advantages and limitations to the program presented in this study. This environment can be used effectively for any generic configuration without limitation to any specific shape unlike various other traditional programs. Though the run times have not been thoroughly compared, the run time of the present method is expected to be slightly more than other methods. This code is supposed to produce higher fidelity results because some assumptions and approximations of previous methods have been overcome and the definition of the aircraft supplied to the code has been improved. The main drawback of the present method is that we are trying to tackle a harder problem and so this method will always be slower than the Harris wave drag program.

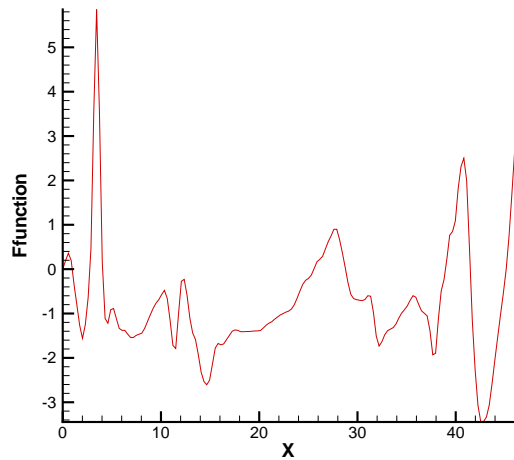


Fig. 18 F-function of F-16 at M=2.0

Future work will include demonstration over a parametric aircraft geometry. The procedure needs to be wrapped in a shape optimization framework with the optimized geometry as the desired output. Work is underway to remove the sharp jumps in the derivative distribution due to the presence of cusps at the intersection of components. The lift analysis can also be coupled with the wave drag analysis to produce a configuration with reduced sonic boom and reduced wave drag. This tool would be particularly useful as a replacement for the traditional Harris wave drag program, AWAVE, and would result in a better prediction of sonic boom analysis in the initial design stages.

Acknowledgments

The authors wish to acknowledge the NASA Langley Research Center and the technical monitor Mr. Robert McKinley for sponsorship of this research under the grant “Design Methodology for Revolutionary Aerospace Concepts”, NAG-1-02023. This work would not have been possible without the valuable contributions and suggestions from Mr. Robert McDonald. We would also like to thank Mr. Stephane Popinet for his prompt replies to our emails and for developing GTS.

References

- ¹Harris, Roy V., Jr. “An Analysis and Correlation of Aircraft Wave Drag”, NASA TM X-947, 1964
- ²Middleton, Wilbur D., Carlson, Harry W., “Numerical Method of Estimation and Optimizing Supersonic Aerodynamic Characteristics of Arbitrary Planform Wings”, Journal of Aircraft, Vol. 2, No. 4, July-Aug., 1965, pp. 261-265
- ³Mack, Robert J., “A Numerical Method for Evaluation and Utilization of Supersonic Nacelle-Wing Interference”, NASA TN D-5057, Nov. 1968
- ⁴Hayes, Wallace D., Haefeli, Rudolph C., Kulrud, H.E., “Sonic Boom Propagation in a Stratified Atmosphere with Computer Program”, NASA CR-1299, 1969
- ⁵Whitham, G., “The flow pattern of a supersonic projectile”, Commun. Pure Appl. Math. V, 301-348, 1952.

⁶Walkden, F., “The Shock Pattern of a Wing-Body Combination, Far From the Flight Path”, Aeronautical Quarterly, vol IX, part 2, May 1958

⁷R. Seebass, “Sonic Boom theory”, Journal of Aircraft, Vol.6, 1969, pp 177-184.

⁸Carlson, H.W., and Maglieri, D.J., “Review of Sonic-Boom generation theory and prediction methods”, Second Sonic Boom Symposium, J. Acoustical Society of America, Vol. 51, No. 2 (Part 3), pp. 675-685, 1972.

⁹Seebass, R., A. R., George, A. R., “Sonic Boom Minimization”, Proceedings of Second Sonic Boom Symposium, J. Acoustical Society of America, Vol. 51, No. 2 (Part 3), pp. 686-694, 1972

¹⁰Seebass, R., Argrow, B., “Sonic Boom Minimization Revisited”, 2nd AIAA Theoretical Fluid Mechanics Meeting, June 15-18, 1998, Albuquerque

¹¹GTS website, <http://gts.sourceforge.net/>

¹²Ashley, Holt, Landahl, Marten, “Aerodynamics of Wings and Bodies”, Dover Publications, 1965.